

Design of Compensators to Relocate Sampling Zeros of Digital Control Systems for DC Motors

Takuya SOGO* and Masafumi JOO**

Abstract: This paper presents a design method for a pre-filter for relocating sampling zeros based on the Taylor expansion, which was recently found to be reduced to a simple formula for a relative degree of 2. The method is successfully applied to sampled-data systems of a DC motor, which usually has a sampling zero near -1 that makes it difficult to apply feedforward control based on pole-zero cancellation. We experimentally demonstrate that the discrete-time model following controller works well and is free from oscillations or ringing for sampled-data systems of a DC motor when the proposed zero-relocation filter is implemented as an analog circuit for an operational amplifier connected to a power amplifier. We also experimentally demonstrate that an analog filter can be replaced by a fast digital filter.

Key Words: sampling zero, feedforward control, digital control, model following control, motor control, multi-rate sampled-data system

1. Introduction

Recently, control systems for various mechanical applications have generally been digital systems. While such systems are continuous-time systems having samplers and zero-order holds (ZOH) with the same time period, they are essentially hybrids of continuous- and discrete-time systems. The conventional approach for analyzing and designing such systems is based on the theory for discrete-time systems that describes the values of the system variables at the sample time. Although the theory for linear discrete-time systems is largely compatible with that for linear continuous-time systems, some critical theoretical relationships are ambiguous. One such relationship is the correspondence of the zeros of transfer functions. We consider the following transfer function of a DC motor:

$$G(s) = \frac{421.8}{s(s + 6.4)}. \quad (1)$$

Applying the ZOH and sampler with the sample time $\tau = 0.01$, gives the pulse transfer function for the sampled-data system as

$$H(z) = \frac{0.0206(z + 0.9789)}{(z - 1)(z - 0.9379)}. \quad (2)$$

While the poles of the pulse transfer function at 1 and 0.9379 respectively correspond to the continuous-time poles at 0 and -6.4 , the pulse transfer function has a discretization zero at -0.9789 , which does not correspond with any continuous-time zero. To complicate matters, because the zero at -0.9789 is very close to -1 , feedforward compensation based on pole-zero cancellation generates persistent oscillations in the output and consequently undesirable oscillations in the mechanical system.

In various control applications, the transfer functions of sampled-data systems often have unstable zeros, which make

it difficult to apply feedforward control based on pole-zero cancellation to such systems. One possible approach for overcoming this difficulty is to relocate the sampling zeros by adjusting the system parameters. In fact, a general continuous-time system described by

$$G(s) = \frac{K(s - q_1) \cdots (s - q_m)}{(s - p_1)(s - p_2) \cdots (s - p_n)} \quad (3)$$

leads to the sampled-data system

$$H_\tau(z) = \frac{C_\tau \{z - \gamma_1(\tau)\} \cdots \{z - \gamma_{n-1}(\tau)\}}{(z - e^{p_1\tau})(z - e^{p_2\tau}) \cdots (z - e^{p_n\tau})} \quad (4)$$

whose poles and zeros are functions of the parameters of $G(s)$. However, in contrast to the poles, there is no simple relation between the m continuous-time zeros $\{q_1, \dots, q_m\}$ and the $n - 1$ sampling zeros $\{\gamma_1(\tau), \dots, \gamma_{n-1}(\tau)\}$, which are generally not expressed by closed formulae of the parameters of the continuous-time transfer function. Hence, to the best of our knowledge, no versatile methods have been reported for adjusting the parameters to relocate sampling zeros. The Taylor expansion of sampling zeros is partially given by

$$\gamma_k(\tau) = 1 + q_k\tau + \frac{q_k^2\tau^2}{2} + O(\tau^3) \quad (5)$$

for $k = 1, \dots, m$ [4]. The Taylor expansion of the other $n - m - 1$ sampling zeros has recently been derived [8]. Moreover, it was demonstrated that the Taylor expansion coefficients can be expressed by simple formulae for the case $n - m = 2$, which implies that it should be possible to approximately relocate the sampling zeros in this case [8]. In this paper, we consider DC motor models as typical examples of this case and develop a pre-filter for relocating sampling zeros. The effectiveness of this approach is demonstrated by experiments of model following control of a DC motor with the relocation pre-filter.

2. Taylor Expansion of Sampling Zeros and Approximate Relocation of the Zeros

* Department of Mechanical Engineering, Chubu University, Aichi 487-8501, Japan

** Nitta Corporation, Osaka 556-0022, Japan

E-mail: sogo@isc.chubu-u.ac.jp

(Received xxx 00, 2011)

(Revised xxx 00, 2011)

2.1 Taylor Expansion of Sampling Zeros for the General Case

The zeros of the pulse transfer function tend to be 1 or the zeros of the so-called Euler–Frobenius polynomial $B_{n-m}(z)$ [1],[9], namely,

$$H_\tau(z) \rightarrow \frac{K\tau^{n-m}(z-1)^m B_{n-m}(z)}{(n-m)!(z-1)^n} \tag{6}$$

as the sample time $\tau \rightarrow 0$, where $B_k(z)$ is defined as

$$B_k(z) = b_1^k z^{k-1} + b_2^k z^{k-2} + \dots + b_k^k \tag{7}$$

and

$$b_j^k = \sum_{l=1}^j (-1)^{j-l} l^k \binom{k+1}{j-l}. \tag{8}$$

Moreover, the Taylor expansion with respect to the sample time τ of the numerator of the pulse transfer function $H_\tau(z)$ and the zero $\gamma_k(\tau)$ that tends to the zero of the Euler–Frobenius polynomial $B_{n-m}(z)$ has recently been derived [8].

Theorem 1 [8] Assume that $G(s)/s$ has simple poles¹ and let r_l be the residue of the continuous-time transfer function $G(s)$ at pole p_l (i.e., $r_l = \lim_{s \rightarrow p_l} G(s)/(s - p_l)$). The pulse transfer function can then be expressed as

$$H_\tau(z) = \frac{\tau^{n-m} \{F_0(z) + F_1(z)\tau + \dots + F_\mu(z)\tau^\mu + \dots\}}{(z - e^{p_1\tau})(z - e^{p_2\tau}) \dots (z - e^{p_n\tau})}, \tag{9}$$

where

$$F_\mu(z) = \frac{1}{(n-m+\mu)!} \sum_{j=1}^n c(\mu, j) (-1)^j z^{n-j} \tag{10}$$

and

$$c(\mu, j) = \sum_{l=0}^n r_l \sum_{\substack{\text{for all combinations of } j \text{ numbers} \\ \{i_1, \dots, i_j\} \text{ chosen from} \\ \{0, 1, \dots, n\} \setminus \{l\}}} (p_{i_1} + \dots + p_{i_j})^{n-m+\mu}. \tag{11}$$

The sampling zero that tends to the zero of the Euler–Frobenius polynomial denoted by λ has the Taylor expansion

$$\gamma(\tau) = \lambda + \alpha_1\tau + \frac{\alpha_2}{2!}\tau^2 + \frac{\alpha_3}{3!}\tau^3 + \dots + \frac{\alpha_\mu}{\mu!}\tau^\mu + \dots, \tag{12}$$

where

$$\alpha_1 = - (F'_0(\lambda))^{-1} F_1(\lambda), \tag{13}$$

$$\alpha_2 = - (F'_0(\lambda))^{-1} \{ \alpha_1 F''_0(\lambda) + 2\alpha_1 F'_1(\lambda) + 2F_2(\lambda) \}, \tag{14}$$

$$\alpha_3 = - (F'_0(\lambda))^{-1} \{ 3\alpha_1\alpha_2 F''_0(\lambda) + \alpha_1^3 F_0^{(3)}(\lambda) + 2\alpha_2 F'_1(\lambda) + (3\alpha_1^2 + \alpha_2) F''_1(\lambda) + 6\alpha_1 F'_2(\lambda) + 6F_3(\lambda) \}, \tag{15}$$

⋮

$$\alpha_\mu = - (F'_0(\lambda))^{-1} \left\{ \sum_v \alpha_{i_1} \dots \alpha_{i_v} F_0^{(j)}(\lambda) + \sum_{k=1}^{\mu-1} k! \sum_v \alpha_{i_1} \dots \alpha_{i_v} F_k^{(j)}(\lambda) + \mu! F_\mu(\lambda) \right\}, \tag{16}$$

¹ This assumption does not restrict the range of applications. For example, if the function has a pole of order 2, one can consider two simple poles, p and $p + \epsilon$ where ϵ is a small number [8].

$$i_1 + \dots + i_v = \mu, i_1 < \mu, \dots, i_v < \mu, j \geq 1, i'_1 + \dots + i'_v = \mu - k, j' \geq 1. \blacksquare$$

It should be noted that

$$F_0(z) = K(z-1)^m B_{n-m}(z) \tag{17}$$

and all the zeros of the Euler–Frobenius polynomial $B_{n-m}(z)$ are real, negative, and distinct, which implies $F'_0(\lambda) \neq 0$. Moreover, for the case $m = 1$, we have $F'_0(1) \neq 0$ and the Taylor expansion (12) is also valid for $\lambda = 1$.

2.2 Taylor Expansion for the Case $n - m = 2$

Although the expressions in Theorem 1 are generally not very simple, it has been demonstrated that for $n - m = 2$ the polynomial $F_\mu(z)$ and the expansion coefficients (12) reduce to relatively simple expressions [8]. Here, we consider

$$G_0(s) = \frac{1}{(s - p_1)(s - p_2)}, \tag{18}$$

which is the main model used in various control applications, such as DC motors. Moreover, to introduce adjustable parameters into (18) while maintaining $n - m = 2$, we add a single pole and a zero to (18), namely,

$$G(s) = \frac{s - q}{(s - p_1)(s - p_2)(s - p_3)}, \tag{19}$$

which leads to the pulse transfer function

$$H_\tau(z) = \frac{C_\tau \{z - \gamma_1(\tau)\} \{z - \gamma_2(\tau)\}}{(z - e^{p_1\tau})(z - e^{p_2\tau})(z - e^{p_3\tau})}, \tag{20}$$

where $\lim_{\tau \rightarrow 0} \gamma_1(\tau) = -1$ and $\lim_{\tau \rightarrow 0} \gamma_2(\tau) = 1$. The expressions in Theorem 1 for $\lambda = -1$ reduce to the following simple expressions [8]:

$$F_0(z) = \frac{1}{2!} (z^2 - 1), \tag{21}$$

$$F_1(z) = \frac{1}{3!} \{ (p_1 + p_2 + p_3 - q)z^2 + (p_1 + p_2 + p_3 - 4q)z - 2(p_1 + p_2 + p_3) - q \}, \tag{22}$$

$$F_2(z) = \frac{1}{4!} \left[\{ p_1^2 + p_2^2 + p_3^2 + p_1 p_2 + p_2 p_3 + p_3 p_1 - (p_1 + p_2 + p_3)q \} z^2 + 2(p_1 + p_2 + p_3)(p_1 + p_2 + p_3 - 4q)z - \{ 3(p_1^2 + p_2^2 + p_3^2) + 5(p_1 p_2 + p_2 p_3 + p_3 p_1) + 3(p_1 + p_2 + p_3)q \} \right], \tag{23}$$

$$F_3(z) = \frac{1}{5!} \left[\{ -(p_1^3 + p_2^3 + p_3^3) - p_1 p_2 p_3 - p_1 p_2 (p_1 + p_2) - p_2 p_3 (p_2 + p_3) - p_3 p_1 (p_3 + p_1) + (p_1^2 + p_2^2 + p_3^2 + p_1 p_2 + p_2 p_3 + p_3 p_1)q \} z^2 + \{ 3(p_1^3 + p_2^3 + p_3^3) + 13p_1 p_2 p_3 + 8p_1 p_2 (p_1 + p_2) + 8p_2 p_3 (p_2 + p_3) + 8p_3 p_1 (p_3 + p_1) - 13(p_1^2 + p_2^2 + p_3^2)q - 18(p_1 p_2 + p_2 p_3 + p_3 p_1)q \} z + 4(p_1^3 + p_2^3 + p_3^3) + 14p_1 p_2 p_3 + 9p_1 p_2 (p_1 + p_2) + 9p_2 p_3 (p_2 + p_3) + 9p_3 p_1 (p_3 + p_1) + 6(p_1^2 + p_2^2 + p_3^2)q + 11(p_1 p_2 + p_2 p_3 + p_3 p_1)q \right]. \tag{24}$$

Substituting these expressions into (13), (14) and (15), we have

$$\gamma_1(\tau) = -1 + \alpha_1\tau + \frac{\alpha_2}{2!}\tau^2 + \frac{\alpha_3}{3!}\tau^3 + \dots, \quad (25)$$

$$\alpha_1 = -(p_1 + p_2 + p_3 - q)/3, \quad (26)$$

$$\alpha_2 = -(p_1 + p_2 + p_3 - q)^2/3^2, \quad (27)$$

$$\begin{aligned} \alpha_3 = & -7(p_1^3 + p_2^3 + p_3^3) \\ & - 27(p_1^2p_2 + p_1^2p_3 + p_1p_2^2 + p_1p_3^2 + p_2^2p_3 + p_2p_3^2) \\ & - 42p_1p_2p_3 + 32(p_1p_2 + p_2p_3 + p_3p_1)q \\ & + 22(p_1^2 + p_2^2 + p_3^2)q - 5(p_1 + p_2 + p_3)q^2 - 10q^3. \end{aligned} \quad (28)$$

Moreover, since the limit of the other sampling zero $\gamma_2(\tau)$, which is at 1, is not a multiple root of $F_0(z)$ and hence $F'_0(1) \neq 0$, the Taylor expansion of $\gamma_2(\tau)$ is also given by (12) in Theorem 1. This leads to

$$\gamma_2(\tau) = 1 + q\tau + \frac{q^2}{2!}\tau^2 + \frac{(p_1 + p_2 + p_3 + 2q)q^2}{6}\tau^3 + \dots. \quad (29)$$

2.3 Approximate Relocation of Zeros Based on Truncation

From (25) and (29) and neglecting the higher-order terms of the expansions, we expect to be able to approximately manipulate the locations of the sampling zero $\gamma_1(\tau)$ and $\gamma_2(\tau)$ in (20) by adjusting the values of the extra zero q and pole p_3 . Here, we truncate (25) and (29) up to the second-order term and minimize the absolute values of the zeros $\gamma_1(\tau)$ and $\gamma_2(\tau)$ to be canceled by the poles of feedforward controller. This results in a stable response with a rapid decay. The absolute values of truncated (25) and (29), namely,

$$\left| -1 - \frac{p_1 + p_2 + p_3 - q}{3}\tau - \frac{(p_1 + p_2 + p_3 - q)^2}{3^2}\frac{\tau^2}{2} \right|, \quad (30)$$

$$\left| 1 + q\tau + q^2\frac{\tau^2}{2} \right| \quad (31)$$

are minimized to 1/2 by choosing

$$q = -1/\tau, \quad (32)$$

$$p_3 = -4/\tau - (p_1 + p_2). \quad (33)$$

Here, as a case study of the approach proposed above, we apply it to the model for the DC motor; i.e., we consider

$$\bar{G}(s) = \frac{1}{s(s-p)} \cdot \frac{s+1/\tau}{s+4/\tau+p} \quad (34)$$

and evaluate the accuracy of the above approximate minimization. From numerical calculations for randomly selected (τ, p) , it was demonstrated that the real values of the sampling zeros $\gamma_1(\tau)$ and $\gamma_2(\tau)$ derived from (34) are solely characterized by the value τp , as depicted in Fig. 1, which shows 10,000 random examples for $(\tau, p) \in [0.0001, 0.1] \times [-200, -0.1]$. From those numerical examples, we found that for values of pole p and sample time τ that do not make τp too small, the modified DC motor model (34) is effective for relocating the sampling zeros to about $\pm 1/2$.

3. Experiment of Model Following Control

To demonstrate the effectiveness of the relocation technique proposed in the previous section, we apply the approach to a digital model following control for an experimental DC motor.

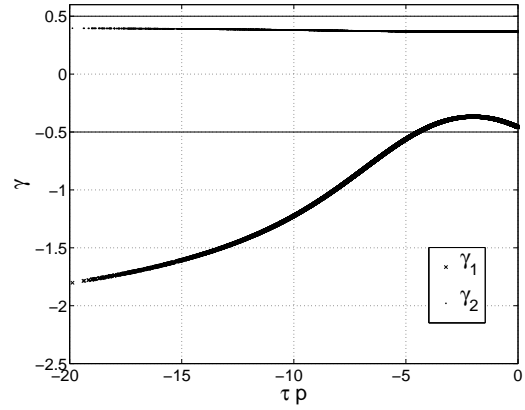


Fig. 1 Examples of values of sampling zeros.

3.1 Experimental Setup of DC Motor

We consider a DC motor with the power amplifier depicted in Fig. 2, the continuous-time model from the input e [V] of the amplifier to the angle θ [rad] of the inertial load is identified as (1), which was given in the Introduction. Applying the ZOH

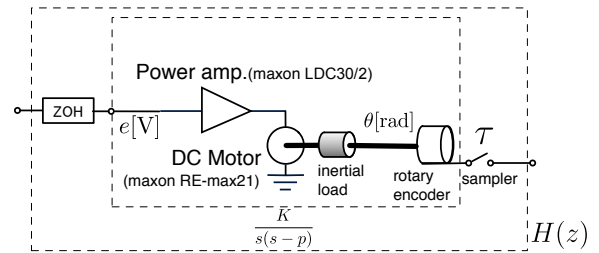


Fig. 2 Experimental setup.

and a sampler with a sample time $\tau = 0.01$ s to the DC motor system depicted in Fig. 2, we have the pulse transfer function (2), which has a zero at -0.9789 . To relocate this zero, we apply the method developed in the previous section to the transfer function (1), namely the addition of a single pole and zero described by (34). We have

$$\bar{G}(s) = \frac{421.8}{s(s+6.41)} \cdot \frac{s+100}{s+393.6}. \quad (35)$$

The value of $\tau p = -0.0641$ is not too small to approximately relocate the zeros to around $\pm 1/2$ (see Fig. 1); the scalar 421.8 is independent of the location of the zeros and poles. Consequently, the transfer function (35) leads to the pulse transfer function

$$\bar{H}(z) = \frac{0.011093(z+0.4519)(z-0.3681)}{(z-1)(z-0.9379)(z-0.01953)}, \quad (36)$$

whose zeros can be cancelled by poles that have much shorter decay times than the pulse transfer function (2).

To implement the additional pole and zero for (35), we introduce an operational amplifier circuit, as depicted in Fig. 3, whose transfer function is

$$C(s) = -\frac{C_1}{C_2} \cdot \frac{s+1/(C_1R_1)}{s+1/(C_2R_2)}. \quad (37)$$

Example capacitances and resistances that realize the transfer function (35) are

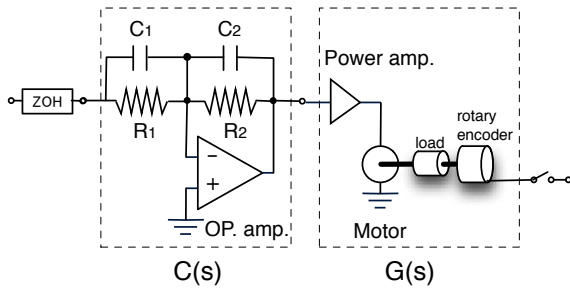


Fig. 3 DC motor system with operational amplifier circuit.

$$C_1 = C_2 = 0.1\mu F, \quad (38)$$

$$R_1 = 100k\Omega, \quad (39)$$

$$R_2 = 25.4k\Omega. \quad (40)$$

3.2 Model Following Control

To demonstrate the effectiveness of the zero relocation, we apply model following control [5] to the modified DC motor system, which fully relies on pole-zero cancellation to cause the output of the objective system to converge to the output of the canonical model.

Consider the discrete-time objective system $\hat{y}(z) = H(z)\hat{u}(z)^2$ with $H(z) = B(z)/A(z)$ where

$$B(z) = b_0z^{n-1} + b_1z^{n-2} + \dots + b_{n-1}, \quad (41)$$

$$A(z) = z^n + a_1z^{n-1} + \dots + a_n, \quad (42)$$

and the canonical model $\hat{y}_M(z) = H_M(z)\hat{u}_M(z)$. Then, the model following control gives an input $\hat{u}(z)$ that makes the output $\hat{y}(z)$ satisfy

$$D(z)(\hat{y}(z) - \hat{y}_M(z)) = 0, \quad (43)$$

where the roots of $D(z)$ are set as appropriate values to adjust the convergent rate of the output error $y(k) - y_M(k)$ to 0 as $k \rightarrow \infty$. Let $D(z) = 1 + d_1z^{-1} + \dots + d_nz^{-n}$ then such input is given by

$$\hat{u}(z) = \frac{1}{b_0} \{D(z)z\hat{y}_M(z) - B_S(z)\hat{u}(z) - R(z)\hat{y}(z)\}, \quad (44)$$

where

$$B_S(z) = b_1z^{-1} + \dots + b_{n-1}z^{-(n-1)}, \quad (45)$$

$$R(z) = (d_1 - a_1) + (d_2 - a_2)z^{-1} + \dots + (d_n - a_n)z^{-(n-1)}, \quad (46)$$

which is depicted by the block diagram in Fig. 4. The feedback

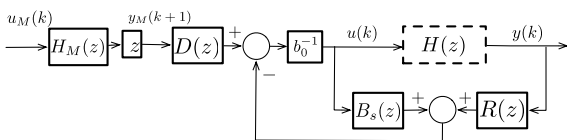


Fig. 4 Model following control

block consisting of b_0^{-1} and $B_S(z)$ in the controller, namely

² $\hat{y}(z)$ and $\hat{u}(z)$ indicate the z-transformed variables of the discrete-time signal $y(k)$ and $u(k)$ ($k = 0, 1, \dots$), respectively. In the following discussions, the time and z-domain signals are described likewise.

$$\frac{b_0^{-1}}{1 + b_0^{-1}B_S(z)} = \frac{1}{b_0 + b_1z^{-1} + \dots + b_{n-1}z^{-(n-1)}} = \frac{z^{n-1}}{B(z)} \quad (47)$$

cancels all the zeros of the objective system $H(z)$ and hence the stability of the zeros is necessary for the stability of the controller.

For the zero-relocated pulse transfer function (36) of the DC motor, we choose the canonical model as

$$H_M(z) = \frac{0.001z^2}{(z - 0.95)^3} \quad (48)$$

and set

$$D(z) = (1 - 0.1z^{-1})^3. \quad (49)$$

Figure 5 shows the experimental results for the above controller with the input

$$u_M(t) = \begin{cases} 1 & (1 \leq t \leq 4) \\ 0 & \text{otherwise.} \end{cases} \quad (50)$$

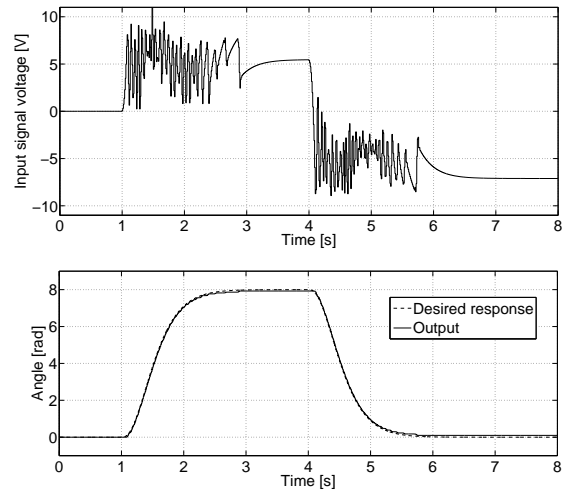


Fig. 5 Input $u(k)$ and output $y(k)$ signals from the motor with relocation filter.

We conducted the same experiment on the DC motor without the filter, namely the pulse transfer function (2) and Fig. 2; we set

$$D(z) = (1 - 0.1z^{-1})^2 \quad (51)$$

corresponding to the transfer function (2) and apply the model following controller (44) with the same canonical model as (48) to the discrete-time model. It should be noted here that although the difference of value for the order n of the denominators in (36) and (2) necessarily causes the difference of the order of (49) and (51), the roots of (49) and (51) are set as the same value, which results in the same convergent rate of the output error $y(k) - y_M(k)$. Figure 6 shows the experimental results obtained without the relocation filter. Although the desired output trajectory is tracked very well by the motor both with and without the relocation filter, the oscillations in the input signal to the DC motor without the relocation filter are sustained much longer than with the filter, as shown in Figs. 5 and 6. Such oscillatory phenomenon is caused by the poles of the controller (47), which originates from the sampling zero near -1 .

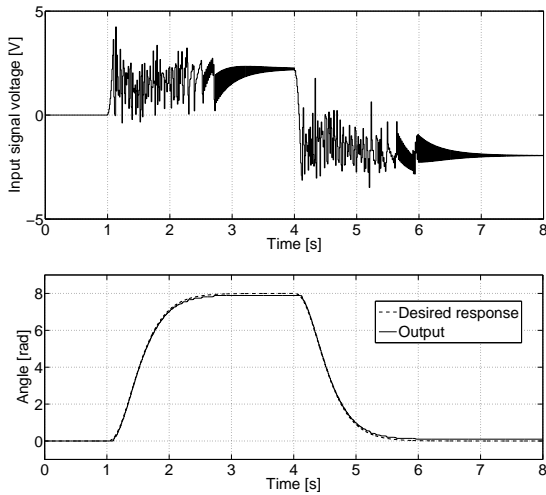


Fig. 6 Input $u(k)$ and output $y(k)$ signals from the motor without the relocation filter.

Moreover, it is often observed that the model following controller without the relocation filter causes the body of the motor to hum loudly and jitter in the angle even after the output of the canonical model settles to the constant value. Such hum and jitter occur frequently in particular when external torque is applied to the motor shaft. Figure 7 shows such an example of the observed phenomenon when a constant torque is applied to the motor shaft by another current-controlled DC motor. (The external torque of 4.92mNm has been applied since 1s.) In contrast, the model following controller with the relocation filter is stable when the output of the canonical model settles to the constant value; any oscillatory phenomenon such as the case without the relocation filter is not observed even when various external torques are applied by the external motor or fingers. Figure 8 shows an example of response of the DC motor with the relocation filter applied by the same external torque as Fig. 7.

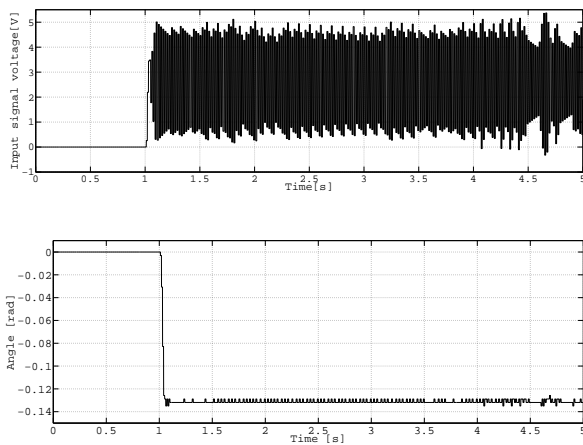


Fig. 7 Input signal and motor angle for the amplifier without the relocation filter (response to the external torque).

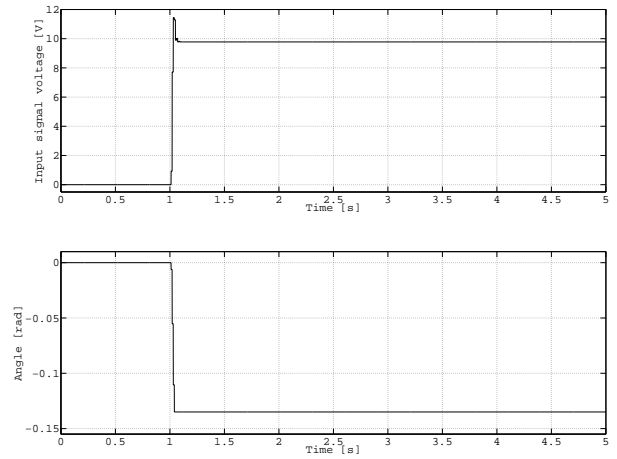


Fig. 8 Input signal and motor angle for amplifier with relocation filter (response to the external torque).

3.3 Substitution of Analog Filter by Fast-Sampling Digital Filter

The zero-relocation filter introduced to the DC motor in the previous section is used to block the lower-frequency component in the step-shaped signals generated by the ZOH, as depicted in Fig. 9. This observation suggests approximating the

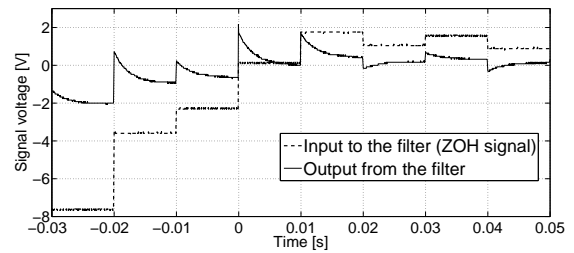


Fig. 9 Input and output of zero relocation filter.

output of the analog relocation filter $(s - q)/(s - p_3)$ by the output of the fast ZOH signal with a time period δ that is sufficiently shorter than the original sample time τ for the ZOH (see the transformation from the upper part to the middle part in Fig. 10)³; this transformation is mathematically validated by the fact that the continuous signal from the analog filter can be approximated by the step-shaped signal from the ZOH with arbitrary accuracy provided the width of the step is sufficiently small [7]. Since a single step of the ZOH signal of the time period τ is a sequence of the τ/δ times repeated steps of the ZOH signal of the time period δ , the ZOH of the time period τ in the middle part of Fig. 10 is virtually replaced by the fast ZOH of the time period δ without loss of accuracy. Finally, the continuous-time filter $(s - q)/(s - p_3)$ connected with the virtual fast ZOH and the sampler of the time period δ leads to the discrete-time filter

$$F(\bar{z}) = (1 - \bar{z}^{-1})\mathcal{Z}_\delta \left\{ \mathcal{L}^{-1} \left[\frac{s - q}{s - p_3} \times \frac{1}{s} \right] \right\}, \quad (52)$$

where $\mathcal{L}^{-1}[\cdot]$ and $\mathcal{Z}_\delta[\cdot]$ indicate the inverse Laplace transform and z-transform of the discrete-time signal obtained by

³ For simplicity, we assume that $\delta = \tau/N$ where N is a natural number.

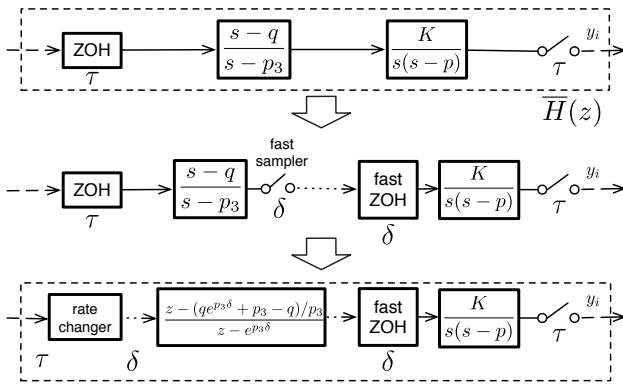


Fig. 10 Substitution of analog relocation filter by digital counterpart.

sampling at the time period δ , respectively [2],[8]. Since $\mathcal{Z}_\delta \{ \mathcal{L}^{-1} [1/(s-p)] \} = \bar{z}/(\bar{z} - e^{p\delta})$, we have

$$F(\bar{z}) = (1 - \bar{z}^{-1}) \left(\frac{(p_3 - q)/p_3 \bar{z}}{\bar{z} - e^{p_3 \delta}} + \frac{q/p_3 \bar{z}}{\bar{z} - 1} \right) \quad (53)$$

$$= \frac{\bar{z} - (qe^{p_3 \delta} + p_3 - q)/p_3}{\bar{z} - e^{p_3 \delta}}. \quad (54)$$

Thus the analog relocation filter with the virtual fast ZOH at the input port and the fast sampler at the output port is substituted by the digital filter (54) with the rate changer that simply repeats the same value for the output for τ/δ times (see the transformation from the middle part to the lower part in Fig. 10). Figure 11 shows an example of the output of the digital relocation filter with the output of the corresponding analog relocation filter.

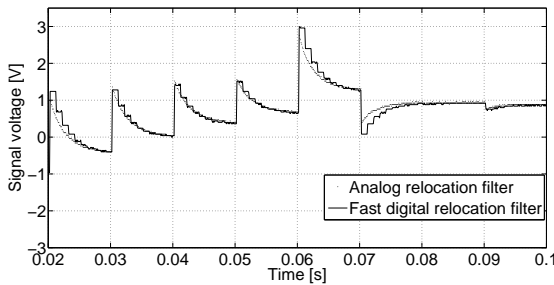


Fig. 11 Approximation of output of the analog relocation filter by fast digital filter with $\delta = \tau/10 = 0.001$.

When we replaced the analog filter of the previous experiment in 3.2 by a digital filter (54) with a sample period $\delta = \tau/10$, we obtained the results shown in Fig. 12, which is similar to those shown in Fig. 5.

This approach provides another design method for multi-rate sampled-data control systems, which has been demonstrated to be effective to design feedforward controller for sampled-data systems with unstable zeros [3],[6].

4. Conclusion

We presented a design method for the pre-filter to relocate sampling zeros based on the Taylor expansion with respect to the sample period. This method was successfully applied to sampled-data systems of a DC motor, which usually has a sampling zero near -1 , hence making it difficult to apply feedforward control based on pole-zero cancellation. An experiment

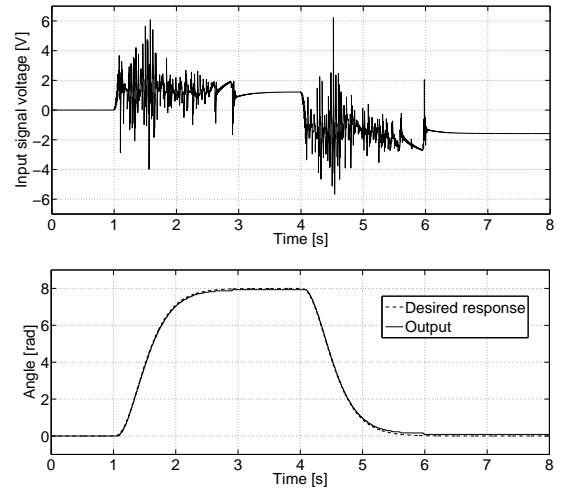


Fig. 12 Input signal generated by the fast ZOH and response of the motor with the digital relocation filter of $\delta = \tau/10 = 0.001$.

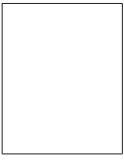
of model following control was performed to demonstrate the effectiveness of the proposed zero-relocation filter for sampled-data systems of a DC motor. It was demonstrated that the analog zero-relocation filter could be replaced by a fast digital filter.

Acknowledgement

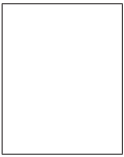
The authors are very grateful to Tomomichi Hagiwara and Toshiharu Sugie for their helpful comments regarding this work. The authors are indebted to Kazuma Date and Masayoshi Tsukada for their assistance with the experiments. This work was supported by Grant-in-Aid for Scientific Research (C) (22560456).

References

- [1] K. J. Åström, P. Hagander, and J. Sternby: Zeros of sampled systems, *Automatica*, Vol.20, No.1, pp31–38, 1984.
- [2] G. F. Franklin, J. D. Powell, and M. L. Workman: *Digital Control of Dynamic Systems*. Addison-Wesley, 1998.
- [3] H. Fujimoto, Y. Hori, and A. Kawamura: Perfect tracking control method based on multirate feedforward control. *Transactions of the SICE*, Vol.36, No.9, pp766–772, 2000 (In Japanese).
- [4] T. Hagiwara and M. Araki: Stability of the limiting zeros of sampled-data systems with zero and first-order holds. *International Journal of Control*, Vol.58, No.6, pp1325–1346, 1993.
- [5] I.D. Landau and M. Tomizuka. *Theory and Practice of Adaptive Control*, Ohmsha, 1981.
- [6] T. Mita, Y. Chida, Y. Kaku, and H. Numasato: Two-delay robust control and its applications – avoiding the problem on unstable limiting zeros, *IEEE Transactions on Automatic Control*, Vol.35, No.8, pp962–970, 1990.
- [7] T. Sogo: Inversion of sampled-data system approximates the continuous-time counterpart in a noncausal framework, *Automatica*, Vol.44, No.3, pp823–829, 2008.
- [8] T. Sogo: Expansion formulae of sampled zeros and a method to relocate the zeros, *Transactions of the SICE*, Vol.46, No.2, pp.91–96, 2010 (In Japanese).
- [9] S. R. Weller, W. Moran, B. Ninness, and A. D. Pollington: Sampling zeros and the Euler-Frobenius polynomials, *IEEE Transactions on Automatic Control*, Vol.46, No.2, pp340–343, 2001.

Takuya Sogo (Member)

He received the B.E., M.E., and Ph.D. degrees in engineering from Kyoto University, Japan in 1990, 1992, and 1999, respectively. From 1995 to 2001, he was an Assistant Professor at the Faculty of Engineering and the Graduate School of Informatics, Kyoto University. Since 2001, he has been affiliated with Chubu University, where he is currently an Associate Professor at the Department of Mechanical Engineering. He held a visiting research position at University of California Santa Barbara, USA in 2007 and 2008. His current research interests are in iterative learning control, sampled-data systems, and feedforward control.

Masafumi Joo

He received the B.E. and M.E. degrees in mechanical engineering from Chubu University, in 2009 and 2011, respectively. He was a member of the robot development team "Owaribito-CU" at Chubu University for Robocup, the international robotics competition. Since 2011, he is with Nitta Corporation in Osaka, Japan.
